

## Video Article

# Image-based Lagrangian Particle Tracking in Bed-load Experiments

Alessio Radice<sup>1</sup>, Sankar Sarkar<sup>2</sup>, Francesco Ballio<sup>1</sup><sup>1</sup>Dept. of Civil and Environmental Engineering, Politecnico di Milano<sup>2</sup>Physics and Applied Mathematics Unit, Indian Statistical InstituteCorrespondence to: Alessio Radice at [alessio.radice@polimi.it](mailto:alessio.radice@polimi.it)URL: <https://www.jove.com/video/55874>DOI: [doi:10.3791/55874](https://doi.org/10.3791/55874)

Keywords: Environmental Sciences, Issue 125, River hydraulics, sediment transport, bed-load, Lagrangian approach, laboratory experiments, image analysis, particle tracking.

Date Published: 7/20/2017

Citation: Radice, A., Sarkar, S., Ballio, F. Image-based Lagrangian Particle Tracking in Bed-load Experiments. *J. Vis. Exp.* (125), e55874, doi:10.3791/55874 (2017).

## Abstract

Image analysis has been increasingly used for the measurement of river flows due to its capabilities to furnish detailed quantitative depictions at a relatively low cost. This manuscript describes an application of particle tracking velocimetry (PTV) to a bed-load experiment with lightweight sediment. The key characteristics of the investigated sediment transport conditions were the presence of a covered flow and of a fixed rough bed above which particles were released in limited number at the flume inlet. Under the applied flow conditions, the motion of the individual bed-load particles was intermittent, with alternating movement and stillness terms. The flow pattern was preliminarily characterized by acoustic measurements of vertical profiles of the stream-wise velocity. During process visualization, a large field of view was obtained using two action-cameras placed at different locations along the flume. The experimental protocol is described in terms of channel calibration, experiment realization, image pre-processing, automatic particle tracking, and post-processing of particle track data from the two cameras. The presented proof-of-concept results include probability distributions of the particle hop length and duration. The achievements of this work are compared to those of existing literature to demonstrate the validity of the protocol.

## Video Link

The video component of this article can be found at <https://www.jove.com/video/55874/>

## Introduction

Since pioneering works appeared some decades ago<sup>1,2</sup>, the use of image analysis for the study of river sediment transport has been constantly increasing. This technique indeed proved its capability to provide relatively high-resolution and low-cost data for detailed analyses of physical phenomena<sup>3,4,5</sup>. With time, significant improvements have been obtained for both hardware and software tools.

The measurement of sediment transport can be performed using a Eulerian approach that targets measurement of sediment fluxes, or a Lagrangian one that aims at measuring trajectories of individual grains as they move. Image processing offers unique possibilities for particle tracking in comparison to other Eulerian methods<sup>6,7</sup>. However, despite these potentialities, the application of image analysis to bed-load sediment transport suffers from some critical experimental limitations, in terms of spatial/temporal support scales for the measurement and size of data samples. For example, it is difficult to achieve simultaneously an appropriate combination of a large spatial area, long duration of an experiment, and high measuring frequency<sup>3,4,8</sup>, without compromising the quality and quantity of data. In addition, the particle tracking can be performed manually<sup>2,4</sup>, which requires a great human effort, or automatically<sup>3,8</sup>, with the possibility of tracking errors made by the software used for the analysis.

This paper presents a protocol for the experimental investigation of bed-load sediment transport, where long duration was achieved by the type of camera used, large field of view was ensured by simultaneous use of two cameras at different locations, and reliable automatic processing was made possible by *ad hoc* experimental conditions. The experimental operation was designed and the processing tools were selected based on experience acquired by the authors in several research works dealing with the detailed investigation of sediment transport by image methods<sup>3,9,10,11,12,13,14,15,16,17,18</sup>.

A sediment transport experiment is described, that was performed releasing particles over a fixed, rough bed. The particle feeding was much less than the transport capacity of the flow to maintain a low concentration of moving grains, thus avoiding the congestion of particles to be tracked. Furthermore, the transported particles were not moving continuously, but intermittent motion was observed. The use of a fixed bed rather than a movable one represents a loss of similarity to natural conditions. However, a fixed bed was frequently used in sediment transport experiments<sup>19,20,21</sup> under the assumption that the results are more simple and explanatory than those from complicated scenarios with a variety of acting processes. The use of a fixed bed obviously prevents processes of sediment burial and reappearance from being observed. On the other hand, in the presence of a weak bed load, the transport of sediment takes place in a superficial layer of a loose bed, and in this case, the use of a fixed bed may be adequate. In fact, specific comparisons between the properties of particle motion in experiments run with the two conditions did not present any significant differences<sup>3,14</sup>. Finally, the experiment presented here was performed with a pressurized flow to ensure an optimal condition for particle visualization through a transparent cover. Sediment transport with a pressurized flow has been experimentally

studied in research prototyping ice-covered rivers, showing that the interaction between the near-bed boundary layer and the sediment is analogous to that of open-channel flow<sup>22,23</sup>. In the following sections, all methods are outlined and some representative results are provided.

## Protocol

Note: The sediment transport experiment was performed in a flume at the Mountain Hydraulics Lab situated in the Lecco campus of the Politecnico di Milano. The flume is completely constructed of transparent acrylic material and is 5.2 x 0.3 x 0.45 m<sup>3</sup>. The channel is supported by two steel beams and can be operated at different slopes because of a hinge and screw jack. A series of lids enable the flume to act as a closed conduit, which was the covered-flow configuration, and the channel employed in this work.

### 1. Measuring and Setting up the Flume Slope

1. Seal the outlet of the flume and fill with still water.  
NOTE: The sealing method will depend on the channel features. In the case presented here, the terminal section of the channel is equipped with a coupling flange, therefore sealing was obtained by bolting a plastic plug to the flange with a rubber washer in between them.
2. Operate the screw jack to set an arbitrary channel slope.
3. Wait at least 30 min to allow the water to achieve stillness. To check the oscillation deadening and achievement of a still-water condition, place a point gauge on the flume walls and repeatedly measure the elevation of the free surface.
4. Place the point gauge on the channel walls at multiple locations and take readings of the elevation of the free surface.  
NOTE: The readings differ from each other as the flume is inclined while the water surface is horizontal.
5. Compute a slope value based on linear interpolation of the readings by the point gauge.
6. Take a measurement with a laser distance sensor that is attached to one of the beams supporting the channel and points to the floor.  
NOTE: Here, the laser sensor is permanently attached to the channel, therefore no operations are required in the protocol for its setup.
7. Repeat steps from 1.2 to 1.6 for a variety of slope conditions.
8. Fit a linear equation to the experimental points in a Cartesian plane with the laser measurement on the horizontal axis and the channel slope measurement on the vertical axis. Determine a transfer function from laser measurement to channel slope (and vice versa).

### 2. Setting up the Working Configuration

1. Prepare a set of steel plates (2-mm thickness) with a total dimension equal to that of the channel bottom.  
NOTE: Here, four plates with a size of 1.3 x 0.3 m<sup>2</sup> were used.
2. Create a fixed rough bed by gluing sediment particles over the plates. To do this, paint the plates with a two-component polyester resin, then spread a layer of sediment (1-1.5 cm) over them.  
NOTE: The sediment particles used here were Polybutylene Terephthalate (PBT) grains, manufactured in white color and with a size of 3 mm. With the procedure above, the thickness of the sediment glued to the plate is similar to the particle size.
3. Wait at least 24 h to allow the resin to dry, then remove the excess sediment by inclining the plates and let the sediment slide away. Paint the sediment surface in black with a water-resistant spray paint. Wait at least 10 h to allow the paint to dry.
4. Place the sediment-coated plates (see steps 2.1-2.3) into the flume and onto Polyvinyl Chloride (PVC) supports to create the bottom of a working section. Pay attention to the placement of consecutive plates to ensure continuity of the bed.  
NOTE: The use of the PVC supports is optional. In the present case, the cross section of the flume (0.3 m wide and 0.45 m high, corresponding to a width-to-depth ratio lower than 1) was originally designed in order to run sediment transport experiments with a layer of loose sediment. The experiment presented in this manuscript was instead run with a fixed bed, leading to unusual, too low values of the width-to-depth ratio. The PVC supports were therefore used in order to achieve a larger value for this ratio.
5. Place a series of transparent acrylic lids (covering the entire channel length) onto the channel walls to create a covered working section.  
NOTE: In the flume described here, the lids are internal boxes with a height of 20 cm, simply laying over the flume walls. Therefore, some water is present at the lid sides during experiments, but does not alter significantly the flow within the flume. The working section used in the experiment presented below was as large as 0.3 m x 0.105 m<sup>2</sup>.

### 3. Establishing Steady Flow Conditions

1. Switch the pump on, fill the channel with water and use the regulation valve to set a flow rate.  
NOTE: In this work, the flow rate was measured by an electro-magnetic flow-meter placed along the delivery pipe.
2. Use a tail-water regulator to set the elevation of the pressure head slightly above the channel lids, ensuring that there is a covered flow but avoiding a significant buoyancy force on the lids.  
NOTE: In the channel presented here, the tail-water regulation is achieved by an array of sticks located at the end of the flume.
3. Repeatedly measure the flow rate and the pressure head to check the stability of the flow conditions.

### 4. Characterizing the Flow Distribution

1. **Measure the vertical profile of the stream-wise velocity component at a variety of locations.**
  1. Place the probe of an ultrasonic velocity profiler (UVP) above the flume lid using an appropriate probe-holder. Place the probe at a chosen inclination with the tail towards the channel inlet. Apply an appropriate ultrasonic coupling gel in the space between the probe tip and the lid to avoid the passage of the ultrasonic wave through air. Connect the probe to its acquisition module.  
NOTE: In the present case, the probe-holder was made of PVC and consisted of a base with an inclined guide attached. This support was constructed after a probe angle was chosen.
  2. Sample several instantaneous velocity profiles.

NOTE: With the instrument used in this experiment, this step required manual setting the frequency of the emitted ultrasound ray, a pulse repetition frequency, a resolution, and the desired number of instantaneous profiles. Profiles were continuously acquired and saved when the desired number was reached.

3. Repeat steps 4.1.1 and 4.1.2, except place the probe with the tail towards the channel outlet.
4. Assess the need for signal de-spiking<sup>24</sup> by a visual inspection of the acquired time evolutions of stream-wise velocity. Perform de-spiking during the data processing if necessary.
5. Compute the average velocity value for each measuring location (gate) of the UVP to obtain time-averaged profiles of the probe-wise velocity component from the two measurements (with the tail of the probe towards the channel inlet and outlet).
6. Use a trigonometric composition of the two probe-wise velocities measured at any elevation to obtain the stream-wise and vertical velocity components.
  1. With  $v_{up}$  and  $v_{down}$  as the time-averaged velocities measured in steps 4.1.2 and 4.1.3, respectively, determine the stream-wise ( $u$ ) and vertical velocity ( $v$ ) components as:

$$u = \frac{0.5(v_{up} - v_{down})}{\cos(\alpha)}$$

$$v = \frac{-0.5(v_{up} + v_{down})}{\sin(\alpha)}$$

Where,  $\alpha$  is the inclination of the probe with respect to the channel.

7. Adjust the distance values for the measuring locations in a profile accounting for the different media (gel, acrylic and water) through which the acoustic beam was travelling<sup>25</sup>.
8. Repeat steps from 4.1.1 to 4.1.7 for all the measuring locations.

**2. Measure the shear velocity from the vertical profile of the stream-wise velocity component.**

1. Determine a range of elevations where the profile of the stream-wise velocity component denotes a linear trend in a semi-logarithmic plot (see **Figure 2**).
2. Estimate the shear velocity  $u_s$  from the measured profile by fitting a logarithmic equation as follows:

$$\frac{u(z)}{u_s} = \left(\frac{1}{\kappa}\right) * \ln\left(\frac{z}{z_0}\right)$$

where  $u(z)$  is the time-averaged stream-wise velocity at a certain elevation  $z$  from the bed,  $\kappa$  is the Karman constant equal to 0.4, and  $z_0$  is a hydrodynamic roughness length.

3. Quantify the uncertainty in estimation of the shear velocity<sup>26</sup> as:

$$\left\{ \left[ N * \sum_{j=1}^N (u(z_j) - u_s/\kappa * \ln z_j/z_0) \right] / \left[ (N-2) * \left( \sum_{j=1}^N (\ln z_j/z_0)^2 - \left( \sum_{j=1}^N \ln z_j/z_0 \right)^2 \right) \right] \right\}^{0.5}$$

where  $N$  is the number of values used for the curve fitting and  $j$  is a counter ranging from 1 to  $N$ .

## 5. Performing a Sediment Transport Experiment

1. **Set the desired camera parameters (resolution, frequency). Using supports from the camera manufacturer, attach two action cameras to the lateral walls of the lids facing the channel bottom at two stream-wise locations. Ensure that the focus areas for the two cameras overlap.**
  1. Adjust the camera position and orientation by trial and error. Capture a short video from each camera, watch the videos and change the position or orientation of a camera if the two focus areas do not overlap or the camera view is not well aligned with the flume.  
NOTE: In the present work, the camera was operated at 30 fps with a resolution of 1,920 × 1,080 pixel.
2. Establish a steady flow condition as described in steps 3.1 to 3.3. Feed the white particles (the same as those that were glued and painted black in steps 2.2 and 2.3) into the flow at the flume inlet. Pick a handful of particles and release them (a particle every few seconds), maintaining a low concentration of white particles over the black bed. Keep feeding for the entire duration of the experiment.  
NOTE: A low particle concentration simplifies<sup>17</sup> the tracking process in comparison to situations with a higher concentration<sup>18</sup>. Indeed, the match between one particle in a certain image with the same particle in the subsequent image is based on a search window around the former position of the particle<sup>19,27</sup>; a higher concentration increases the possibility to detect more than one particle in the search window, and in turn leads to mismatches.
3. If the room lights are off, then switch them on as it is necessary to synchronize the cameras. Start shooting by triggering the cameras with the appropriate controls. Switch the room lights off after ensuring that both cameras have started filming.  
NOTE: In this way, the time at which the light was switched off will be clearly recognizable from the history of pixel intensity in the images, thus enabling (with less-than-one-frame precision) the time shift between the two acquired movies to be determined. The visualization cannot of course be made in the dark. In the present work, the experiment used only natural lighting (as a side wall of the room is completely glass-made). If the lighting conditions change significantly during the experiment, the run should be repeated because lighting affects the particle identification and tracking described below.
4. Keep filming for the desired duration (here, 15 min), then stop the cameras.  
NOTE: Representative results are shown in the following for a duration of 100 s.
5. Repeat steps from 5.2 to 5.7 for any other desired hydro-dynamic condition (for example, a different flow rate).  
NOTE: During the experiments described here, some trapped particles were present on the bed after the shooting. They should be removed before another configuration is tested, by lifting the lid, using a brush to remove the particle, and replacing the lid.

## 6. Preprocessing Images

1. Correct the image distortion due to limited lens length by applying a radial transformation to the pixel coordinates and remapping the images. Adjust by trial a calibration factor needed to apply the transformation.

NOTE: Given  $r$  as a distance from any pixel to the image center, a transformed distance can be computed as:

$$r_t = r * \left( \frac{1}{1 + k * r} \right)$$

where  $k$  is the calibration factor that needs to be adjusted by trials<sup>28</sup>, based on a visual inspection of the flume bottom sides, which should appear as straight lines in the images.

2. Determine a linear image conversion from pixel to real distance using targets placed at known distances and at the elevation of the bed, on the lateral walls of the flume.

NOTE: This can be accomplished for example in a programming language (see the **Table of Materials**), using the command *imread* to open an image file, the command *ginput* to click on the targets and obtain their coordinates in pixel, and finding a proportion between the so-determined pixel coordinates and the real ones.

## 7. Identifying and Tracking Particles

NOTE: All of the following operations must be performed for the images collected by both cameras, separately. The identification and tracking of particles were performed using Streams<sup>29</sup>. This software is freely available upon an inquiry to its developer. Streams was already employed by the authors in several experiments for bed-load sediment transport in different conditions<sup>3,16,17,18,28,30</sup>.

1. Import frames by clicking on *Image* → *Create image sequence*. Input the time step between two frames and the image calibration factor. Select the image files to be included in the sequence. Click on *OK*.

NOTE: In the present case, the time interval was 1/30 s (corresponding to the frame rate mentioned in step 5.1) and the image calibration factor was 0.5 mm/pixel.

### 2. Identify particles

1. Produce intensity maps for some randomly selected images in order to find the typical intensity value (over a scale from 0 to 255) for pixels corresponding to white particles.

1. Right-click on the *Image sequence* that was created and select *Open image view*. Holding *Shift*, draw any rectangle over the image. Right-click on the rectangle and select *ShowIntensityMatrix*. Choose a suitable threshold value.

NOTE: In the present case, the threshold was set at 80.

2. Threshold the images based on an intensity value and an expected size of white spots in the binary images.

1. Right-click on the *Image sequence* that was created and select *Open process view*. Click on *New*, select *Filter images pipeline* and click on *OK*. Give the process a name, provide the sequence name and click on *OK*. Double-click on the *filter pipeline*, click on *New*, select *Remove background* and click on *OK*.
2. In the *Process* window, click on *New*, select *Identify particles* and click on *OK*. Select *Single threshold* and click on *OK*. In the *Algorithm* page, input the threshold intensity and limiting spot diameters, then click on *OK*. Select the created processes, click on *Add to pipeline* and then on *Execute*.

NOTE: The spot size here was from 0.5 to 8 mm. The spot size relates to the particle size but also depends on the lighting conditions. In fact, the spot corresponds to the light reflected by a particle rather than to the particle itself.

### 3. Track particles

1. Right-click on the *Particle record* that was created and select *Open image view*.
2. Scroll through frames by clicking on forward and backward arrow buttons. Observe typical particle displacements between consecutive images by moving the cursor over the displayed spots and reading coordinates. Determine an appropriate search window accordingly.
3. Right-click on the *Particle record* that was created and select *Open process view*.
4. Click on *New*, select *PTV analysis pipeline* and click on *OK*. Give the process a name and click on *OK*. Double-click on the *PTV analysis pipeline*, click on *New*. In the *Costings* page, select *Distance*. In the *Optimization* page, input the stream-wise and transverse position and the dimension of the search window, and click on *OK*.
5. Select the created process, click on *Add to pipeline* and then on *Execute*.

NOTE: A particle track must ideally reach the end of the focus area or the final experimental time. Similarly, it must start at the beginning of the focus area or at the initial time. However, measured tracks can be unexpectedly interrupted, typically because a particle is not detected in some frames due to a low intensity or less often, due to missed particle match between two successive frames. If the track ends without reaching the boundaries of the time-space observation window, candidates for reconnection can be searched; select ones at a location close to and soon after the end of the last frame before the interruption. In this way, a single track for a particle can be reconstructed as detailed in step 7.3.6.

6. If interruptions are present in the measured tracks, fix them by track reconnection using a search window devoted to that purpose.
  1. Right-click on the *Particle record* that was created and select *Open process view*. Click on *New*, select *Create Lagrangian path field* and click on *OK*. Click again on *OK*. Add the process to the pipeline and click on *Execute*.
  2. Right-click on the *Particle record* that was created (the second one) and select *Open process view*. Click on *New*, select *Join Lagrangian paths* and click on *OK*. In the *Parameters* page, input the details of the search window and click on *OK*. Add the process to the pipeline and click on *Execute*.

- Right-click on the *Particle record* that was created (the second one) and select *Save paths to text file*. Input path and file name, then click on *OK*.

## 8. Joining Trajectories from Different Cameras

NOTE: This is a necessary operation to take advantage from the use of multiple cameras to enlarge the size of the measuring area. Steps are performed by a MatLab code (*join\_cameras.m*) with Graphical User Interface developed by the authors (see **Supplemental Code Files**).

- Browse the computer folders and find track files for both cameras and click on *Find track properties*.
- Make the  $(x,y)$  reference of the two cameras uniform by applying a translation of coordinates to the data from the downstream camera. Determine the constants to be used for translation along the two directions from the targets that are visible in the images from both cameras. Input the required values and click on *Make reference system uniform*.  
NOTE: Until this point, an independent reference is used for cameras with  $(0,0)$  at the lower-left corner of the images, x-axis rightwards and y-axis upwards. The translation of coordinates used in this work was 760.15 and -1.5 pixel in stream-wise and transverse direction, respectively.
- Determine the area of overlap between the two data and input its limits in the appropriate text boxes.  
NOTE: The length of overlap in this work was from 760.15 to 880.11 pixel in the stream-wise direction, and covered the entire channel width.
- Remove from the samples all the trajectories that are shorter than the length of the overlapping area, in order to limit the analysis to simple situations (see **Figure 1**). Input a threshold length in the related text box and click on *Remove shorter than or equal to (mm)*.
- Join tracks**
  - Merge the particle track databases from the two cameras by clicking on *Merge tables*. Input requested values for tolerance of overlap (here, 10 mm) in the stream-wise and transverse directions and click on *JOIN*.  
NOTE: After clicking on *JOIN*, perform the following operations. Scroll the tracks until finding a track ending in the area of overlap. Search candidates for joining, among tracks starting in and exiting the overlapping area. If a candidate is found, compare the times for which the two tracks are within the area of overlap. If these time periods agree with each other, compute the differences between the particle coordinates in the two tracks at all the possible points. Take the square root of the mean squared difference of  $x$  and  $y$  values for the value of the potential for the two particle tracks to be equal. If this indicator is lower than a threshold value, join the tracks. Construct a new track corresponding, in the overlapped portion, to the average of the two previous ones. Repeat all these operations until no new joints are possible. The threshold value used in this work was 10 mm in both directions.
- Name the result file and save the joined tracks by clicking on *Save joined tracks*.

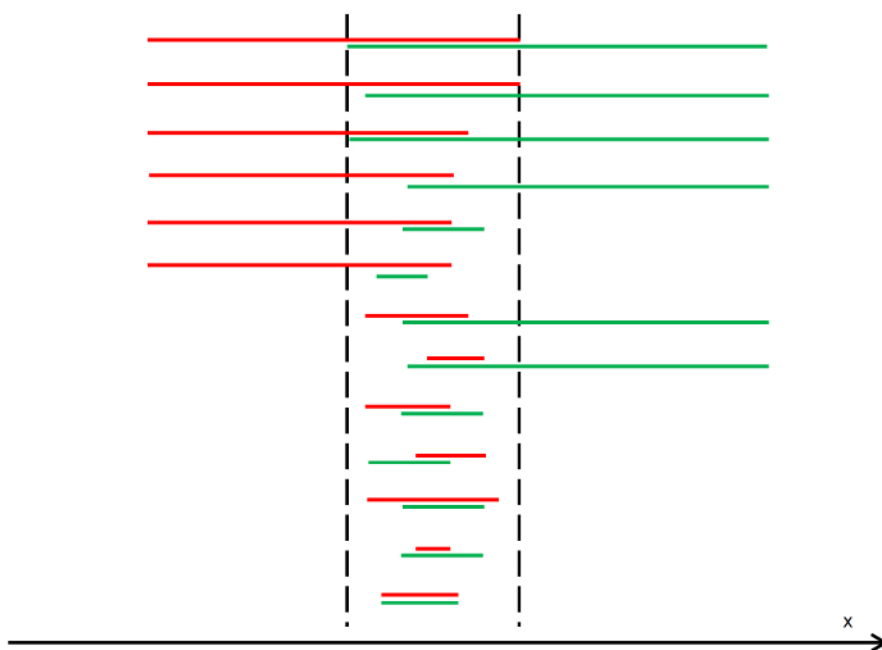


**Figure 1. Situations for Track Joining.** The tracks from the upstream camera are in red and from the downstream camera are in green (one-dimensional representation for the sake of simplicity). The vertical dashed lines bound the nominal length of overlap. Due to possible interruption of tracks, the variety of outcomes is larger than that for expected straightforward tracks (corresponding to the first four sketched cases) with a track from the first camera reaching the overlapping region and a track from the second camera leaving it. A total number of 13 theoretically possible situations is presented. To simplify the analysis, tracks shorter than the length of the overlapping regions are excluded from the preliminary data. [Please click here to view a larger version of this figure.](#)

## 9. Analyzing the Sediment Transport Kinematics

1. Starting from the obtained data set that contains the track of each transported particle, expressed in terms of the  $(x,y)$  position taken at any time point, perform a variety of statistical analyses for a depiction of the bed-load particle kinematics<sup>3,4,5,8,16,17,18</sup>.

### Representative Results

Results presented in this section are for an experiment where the flume slope was set to zero (slope values were computed with  $\pm 0.05\%$  accuracy). The used sediment was made of PBT particles that were quasi-spherical, with a size  $d = 3$  mm and a density  $\rho_p = 1,270$  kg/m<sup>3</sup>. The experiment was run with a flow rate  $Q = 9.7 \times 10^{-3}$  m<sup>3</sup>/s resulting in a bulk velocity  $U = 0.31$  m/s.

For the velocity measurements with the UVP, a 2 MHz probe was used at 81° inclination. Velocity data were acquired at 20 Hz for 250 s. A representative velocity profile is depicted in **Figure 2**. It was taken at the channel axis and at 4.5 m from the flume inlet, where the flow was fully developed. Some values related to invalid elevations measurements were removed. An asymmetric profile resulted from the different roughness of the plastic lid and sediment bed. The plots also show the portion of the profile used for the estimation of the shear velocity, obtaining  $u_s = 25.9 \pm 1.3$  mm/s. The particle Reynolds number ( $Re_p = u_s \times d / \nu$ , with  $\nu$  as the kinematic viscosity of water) was therefore equal to 78, indicating a transitionally rough regime.

The visualization of sediment transport was performed with two cameras placed at 3.5 m and 4.3 m from the flume inlet. The cameras operated at a frequency of 30 fps and with a resolution of 1,920 x 1,080 pixel. The factor for correction of image distortion was  $k = 0.6$ . After removal of distortion, the image calibration was 1 pixel = 0.5 mm. The length of overlap was from 760.15 to 880.11 mm (where the latter was the length of the focus area of the first camera from its upstream edge). The threshold intensity for particle identification was set to 80 and the expected blob size ranged from 0.5 to 8 mm. The search window for particle tracking was as follows: 1 mm upstream and 7 mm downstream, 4 mm laterally. The search window for reconnection of interrupted tracks was as follows: 1 mm upstream and 31 mm downstream, 16 mm laterally along 4 following frames. The threshold value of the square root of the mean squared difference of  $x$  and  $y$  values between two tracks to be joined was set to 10 mm.

The particle tracks measured using a subset of 3,000 images from each camera (corresponding to 100 s duration) are depicted in **Figure 3**. The database comprehended 37 and 34 tracks from the upstream and downstream camera, respectively. An overlap of the tracks obtained by the two cameras is first proposed and then the resulting full set of tracks is displayed. It is evident that the overlap in the central portion of the measuring area was satisfactory. 12 links were obtained at the end 59 tracks. The longest track spanned the entire observation window with a total length of approximately 1.6 m (more than 530 particle sizes, 15.2 flow depths or 5.3 flume widths), which is very large in comparison to other literature studies where similar analyses were performed<sup>3,4,5,8</sup>.

By taking a Lagrangian framework, the key indicators of particle kinematics are here applied in terms of properties of particle hops. Under an intermittent bed-load transport like the one in this experiment, these hops are motions separated by periods of rest. To detect hops within a full track for a single particle, the identification of particle motion and stillness is a necessary preliminary step. In this work, we applied a criterion<sup>30</sup> that considers a particle in motion at a certain instant if its  $x$  position at that instant is larger than all the previous ones and lower than all the following ones. A total number of 98 hops was obtained from the 59 measured particle tracks. **Figure 4** depicts the obtained Cumulative Frequency Distribution (CFD) for the hop length and duration.

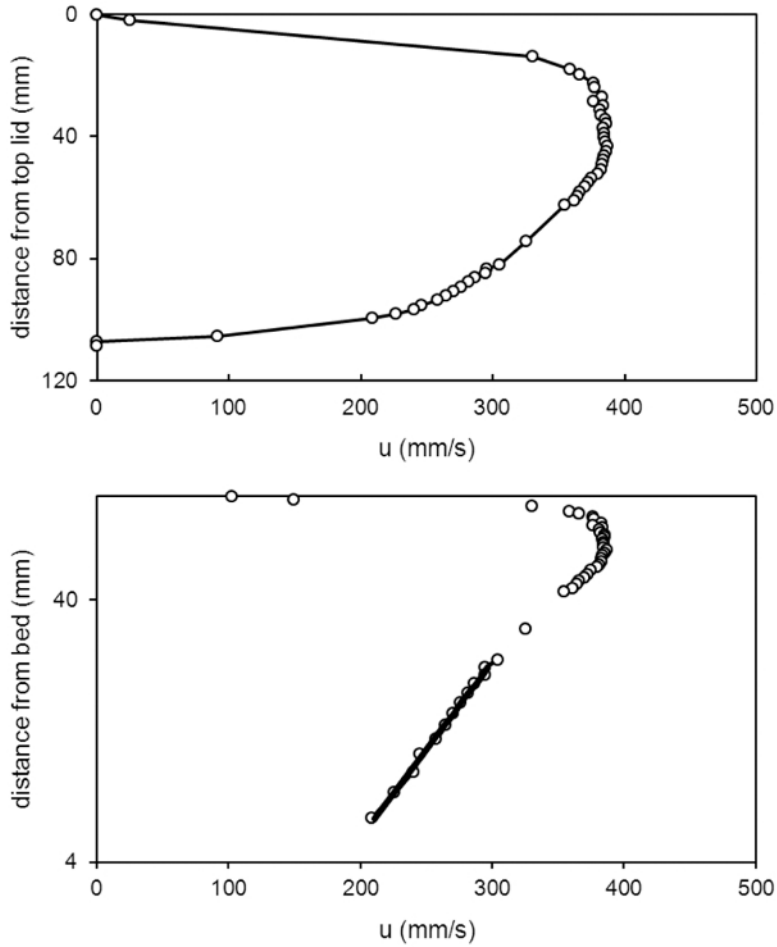


**Figure 2: Measured Velocity Profile.** (Top) The time-averaged vertical profile of the stream-wise velocity component. (Bottom) The estimation of the shear velocity by fitting a logarithmic equation to the lower portion of the profile. Note that a vertical axis starting from the top of the channel and oriented downwards is used in the first plot, representing the result from the measurement with the UVP. An axis from the channel bottom and directed upwards is instead used in the second plot, as needed to estimate the shear velocity by equation fitting. [Please click here to view a larger version of this figure.](#)

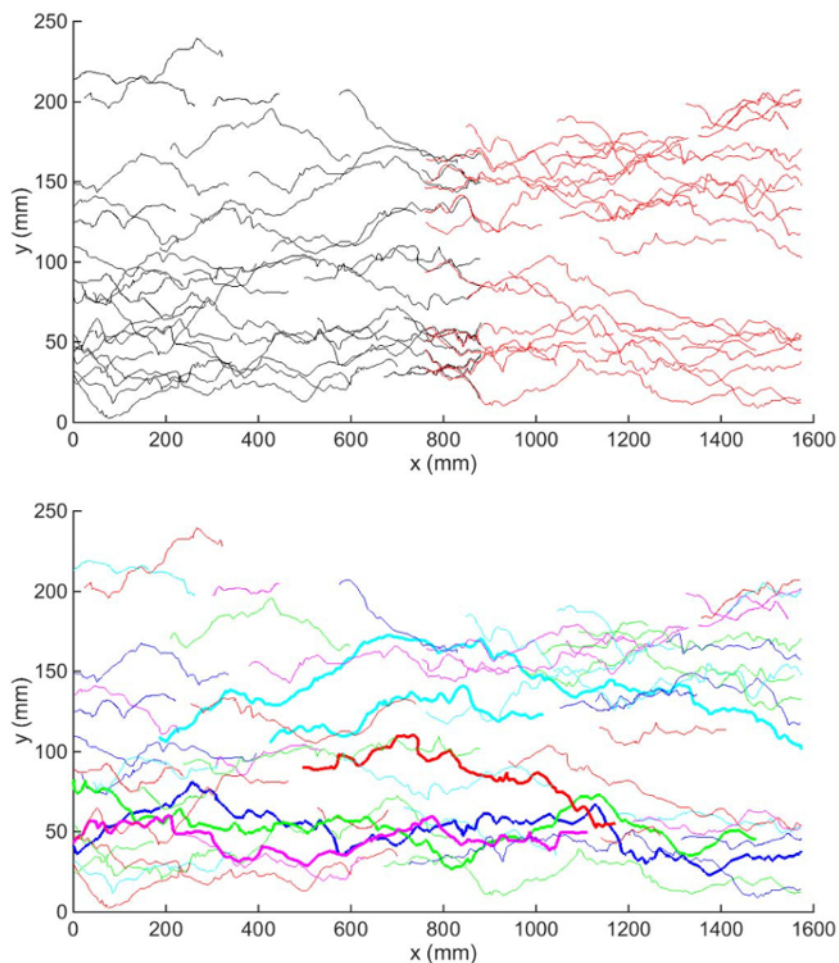


**Figure 3: Plan View of Measured Particle Tracks.** (Top) The tracks from the two cameras (upstream camera in red and downstream in black). (Bottom) The sample of joined tracks (changing color for clarity and some tracks highlighted by a thicker line). [Please click here to view a larger version of this figure.](#)

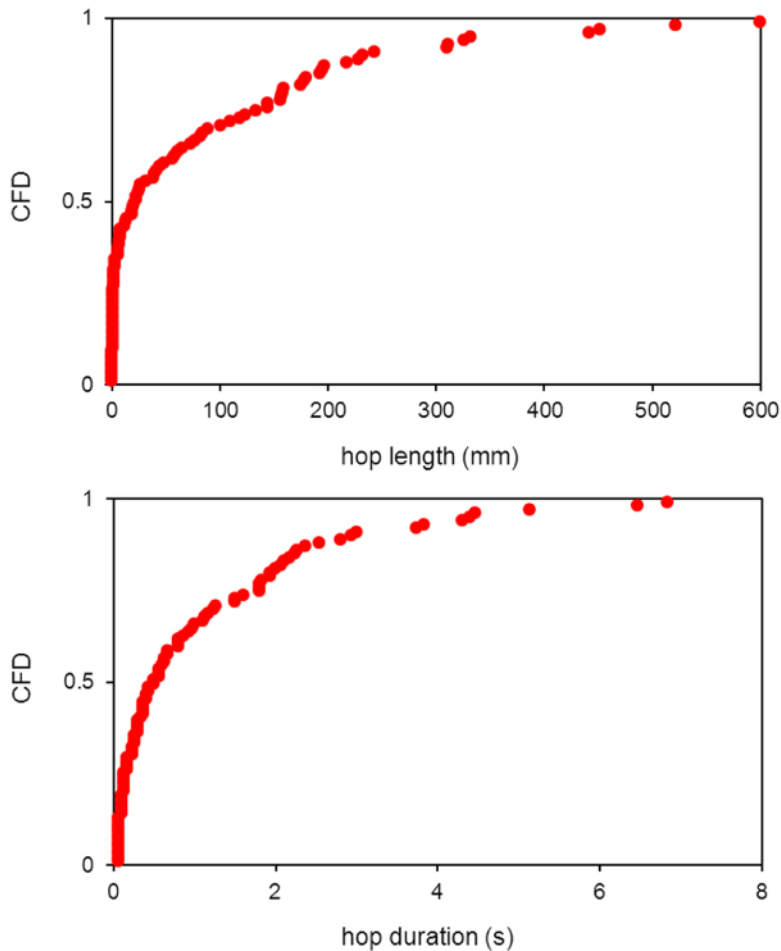


**Figure 4: Cumulative Frequency Distribution (CFD) of Hop Length (Top) and Duration (Bottom).** Within each track of **Figure 3**, the particle was labeled at each time instant to represent if the particle was in motion or at rest at that instant. Particle hops were then extracted from the tracks as portions between particle entrainment (transition from stillness to motion) and disentrainment (transition from motion to stillness). The samples obtained for hop lengths and durations were used to create the distributions depicted here. [Please click here to view a larger version of this figure.](#)

**Supplemental Code Files:** [join\\_cameras.m](#) [Please click here to download this file.](#)

## Discussion

Designing a bed-load transport experiment with particle visualization involves several steps, including the choice of an experimental configuration and hardware tools, flow measurement, particle seeding and visualization, and image analysis. Variations at each step have advantages and disadvantages. The key characteristics of the protocol presented in this manuscript are: (i) using a pressurized flow and a fixed rough bed, (ii) seeding a low number of bed-load particles having a contrasting color to the fixed bed color, (iii) using natural light and, (iv) using multiple cameras to obtain independent track sets to be joined to each other.

The experimental method and the data processing enable the bed-load particles to be reliably tracked for the final measurement. The covered flow guarantees an optimal vision of the moving particles. The fixed bed however, prevents observation of some processes (e.g., those linked with vertical displacements of sediment particles within the active bed-load layer), and thus limits the applicability of the technique to weak bed-loads.

The size of the data samples obtained using only 100 s of movie was relatively small. However, the sample size can easily be increased by lengthening the experimental duration of image acquisition and processing. Feeding a limited number of particles requires a longer experimental time than feeding at a substantially higher rate; but it is well worth the effort because of a relatively straightforward particle tracking due to the small concentration of particles in motion and the use of different colors, both of which reduce the probability of tracking mistakes. The use of natural light in the experiment avoids the need for lighting devices; however, a downside is that good lighting depends on the weather conditions.

The CFDs of particle hop length and duration depicted in **Figure 4** show the lowest values as the most frequent ones. The largest measured values of hop length and duration were around 600 mm and 7 s, respectively. This was significantly larger compared to analogous values from the literature<sup>4,16,30</sup>, since measuring longer tracks runs the risk of long particle hops. The benefit of using two cameras is evident considering that a single camera had a focus area length of around 850 mm, which would not be much larger than hop length values to be measured. The measuring protocol using two cameras instead, ensured a satisfactory separation between the length scales of the process and those of the

measuring field, thus reducing the risk of biasing the phenomenological results due to experimental limitations. Also, the focus area can be additionally lengthened by increasing the number of cameras placed along the flume.

An alternative procedure compared to the protocol described here is to create overlapped images before the particle identification and tracking. Our protocol (of performing the tracking twice and linking particle tracks) was preferred as the image merging method would have doubled the size of the data files, requiring a memory consumption that was not affordable.

With the processing algorithms described here, several particle tracks that were shorter than the length of the overlapping area were discarded because they prevented a full reconstruction of the sediment tracks. However, the threshold length of 120 mm was one order of magnitude shorter than the track lengths that could be obtained, and the loss of these data was therefore acceptable. Moreover, the track joining seen in the lower 8 cases of **Figure 1** would not enable a significant increase in the track length to be obtained. On the other hand, these situations might help in retrieval of long tracks, such as the situation in **Figure 5** that could be due to track interruptions. In a similar case, a long track could be reconstructed by iterative joining operations. It is however important to keep in mind that track interruptions like those in **Figure 5** are clearly related to the tracking process rather than to the joining process.

This manuscript presented proof-of-concept results for a single experiment in order to demonstrate the capabilities of the adopted protocol. In future experiments, the protocol will be applied to a series of different hydro-dynamic conditions to achieve a detailed analysis of the bed-load sediment transport process.

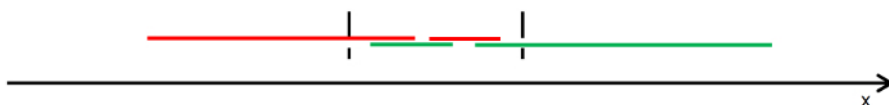


**Figure 5: A Situation of Track Joining in the Presence of Interruptions.** The joining of these tracks into a single track is not possible with the protocol described here. As mentioned in the caption of **Figure 1** and in step 8.4 of the Protocol, the tracks shorter than the length of the overlapping region are excluded. This eliminates the short red and green tracks; therefore, the remaining long ones cannot be joined because they have no common point. [Please click here to view a larger version of this figure.](#)

## Disclosures

The authors declare that they have no competing financial interests.

## Acknowledgements

This work was supported by the Research Executive Agency, through the 7th Framework Programme of the European Union, Support for Training and Career Development of Researchers (Marie Curie - FP7-PEOPLE-2012-ITN), which funded the Initial Training Network (ITN) HYTECH "Hydrodynamic Transport in Ecologically Critical Heterogeneous Interfaces" (number 316546). It was also supported by the Polo Territoriale di Lecco of the Politecnico di Milano. The experiments were performed during a visit by S. S. to the Politecnico di Milano as a visiting scientist. The authors thank Tarcisio Fazzini, Stefania Gherbi, Francesco Mottini (B.Sc. students at the Politecnico di Milano) and Seyed Abbas Hosseini-Sadabadi (fellow of the HYTECH project and Ph.D. student at the Politecnico di Milano) for supporting the experimental activity and the data analysis. The authors gratefully thank Prof. Roger Nokes (University of Canterbury, Christchurch, New Zealand) for providing the Streams software and constant advice. Finally, the authors thank the JoVE managing editor and three anonymous reviewers for their thought-provoking comments and suggestions, thanks to which the manuscript could be significantly improved.

## References

- Francis, J. R. D. Experiments on the motion of solitary grains along the bed of a water-stream. *Proc Royal Soc London, A*. **332**, 443-471 (1973).
- Drake, T. G., Shreve, R. L., Dietrich, W. E., Whiting, P. J., Leopold, L. B. Bedload transport of fine gravel observed by motion-picture photography. *J Fluid Mech.* **192**, 193-217 (1988).
- Campagnol, J., Radice, A., Ballio, F., Nikora, V. Particle motion and diffusion at weak bed load: accounting for unsteadiness effects of entrainment and disentrainment. *J Hydraul Res.* **53**(5), 633-648 (2015).
- Fathel, S. L., Furbish, D. J., Schmeeckle, M. W. Experimental evidence of statistical ensemble behavior in bed load sediment transport. *J Geophys Res: Earth Surf.* **120**(11), 2298-2317 (2015).
- Lajeunesse, E., Malverti, L., Charru, F. Bedload transport in turbulent flow at the grain scale: experiments and modeling. *J Geophys Res: Earth Surf.* **115**, F04001 (2010).
- Tsakiris, A. G., Papanicolaou, A. N., Lauth, T. J. Signature of bedload particle transport mode in the acoustic signal of a geophone. *J Hydraul Res.* **52**(2), 185-204 (2014).
- Mendes, L., Antico, F., Sanches, P., Alegria, F., Aleixo, R., Ferreira, R. M. L. A particle counting system for calculation of bedload fluxes. *Meas Sci Technol.* **27**(12), 125305 (2016).
- Heays, K. G., Friedrich, H., Melville, B. W., Nokes, R. Quantifying the dynamic evolution of graded gravel beds using Particle Tracking Velocimetry. *J Hydraul Eng.* **140**(7), 04014027 (2014).
- Radice, A., Malavasi, S., Ballio, F. Solid transport measurements through image processing. *Exp Fluids.* **41**(5), 721-734 (2006).
- Radice, A., Ballio, F. Double-average characteristics of sediment motion in one-dimensional bed load. *Acta Geophys.* **56**(3), 654-668 (2008).
- Radice, A. Use of the Lorenz curve to quantify statistical nonuniformity of sediment transport rate. *J Hydraul Eng.* **135**(4), 320-326 (2009).
- Radice, A., Ballio, F., Nikora, V. On statistical properties of bed load sediment concentration. *Water Resou. Res.* **45**, W06501 (2009).

13. Radice, A., Ballio, F., Nikora, V. Statistics and characteristic scales for bed load in a channel flow with sidewall effects. *Acta Geophys.* **58**(6), 1072-1093 (2010).
14. Campagnol, J., Radice, A., Ballio, F. Scale-based statistical analysis of sediment fluxes. *Acta Geophys.* **60**(6), 1744-1777 (2012).
15. Radice, A., Nikora, V., Campagnol, J., Ballio, F. Active interactions between turbulence and bed load: Conceptual picture and experimental evidence. *Water Resour Res.* **49**(1), 90-99 (2013).
16. Campagnol, J., Radice, A., Nokes, R., Bulankina, V., Lescova, A., Ballio, F. Lagrangian analysis of bed-load sediment motion: database contribution. *J Hydraul Res.* **51**(5), 589-596 (2013).
17. Ballio, F., Radice, A. Fluctuations and time scales for bed-load sediment motion over a smooth bed. *Int J Sediment Res.* **30**(4), 321-327 (2015).
18. Hosseini-Sadabadi, S. A., Radice, A., Ballio, F. An analysis of entrainment and deposition rate fluctuations in weak bed load transport. In: *Hydrodynamic and mass transport at freshwater aquatic interfaces*. Rowiński, P. M., Marion, A. (eds.), GeoPlanet: Earth and Planetary Sciences, Springer, 333-342 (2016).
19. Papanicolaou, A. N., Diplas, P., Balakrishnan, M., Dancey, C. L. Computer vision technique for tracking bed load movement. *J Comput Civil Eng.* **13**(2), 71-79 (1999).
20. Ramesh, B., Kothiyari, U. C., Murugesan, K. Near-bed particle motion over transitionally-rough bed. *J Hydraul Res.* **49**(6), 757-765 (2011).
21. Amir, M., Nikora, V., Witz, M. A novel experimental technique and its application to study the effects of particle density and flow submergence on bed particle saltation. *J Hydraul Res.* **55**(1), 101-113 (2017).
22. Ettema, R. Ice effects on sediment transport in rivers. In: *Sedimentation Engineering*, M. H. Garcia (ed.), ASCE Manual Rep. on Eng. Pract. No. 110, ASCE, Reston, Va, 613-648 (2008).
23. Knack, I., Shen, H. Sediment transport in ice-covered channels. *Int J Sediment Res.* **30**(1), 63-67 (2015).
24. Goring, D. G., Nikora, V. I. Despiking acoustic Doppler velocimeter data. *J Hydraul Eng.* **128**(1), 117-126 (2002).
25. Nowak, M. Wall shear stress measurement in a turbulent pipe flow using ultrasound Doppler velocimetry. *Exp Fluids.* **33**(2), 249-255 (2002).
26. McCuen, R. H. *Microcomputer applications in statistical hydrology*. Englewood Cliffs, NJ: Prentice Hall (1993).
27. Lloyd, P. M., Ball, D. J., Stansby, P. K. Unsteady surface-velocity field measurement using particle tracking velocimetry. *J. Hydraul. Res.* **33**(4), 519-534 (1995).
28. Radice, A., Aleixo, R., Hosseini-Sadabadi, S. A., Sarkar, S. On image grabbing and processing for measurement of geophysical flows. *Proc. HydroSenSoft 2017*. International Symposium and Exhibition on Hydro-Environment Sensors and Software, Madrid, Spain (2017).
29. Nokes, R. Streams. *System theory and design*. University of Canterbury, Christchurch, New Zealand. <<http://www.civil.canterbury.ac.nz/streams.shtml>> (2016).
30. Hosseini-Sadabadi, S. A., Radice, A., Ballio, F. Post-processing of particle tracking data for phenomenological depiction of weak bed-load sediment transport. *Proc. River Flow 2016*. VIII Int. Conf. on Fluvial Hydraulics, St. Louis, US, 780-786 (2016).